Supplement of Biogeosciences, 13, 6049–6066, 2016
http://www.biogeosciences.net/13/6049/2016/
doi:10.5194/bg-13-6049-2016-supplement

Biogeosciences Open Access EGU

Supplement of

Unveiling the Si cycle using isotopes in an iron-fertilized zone of the Southern Ocean: from mixed-layer supply to export

Ivia Closset et al.

Correspondence to: Ivia Closset (ivia.closset@locean-ipsl.upmc.fr)

Supplementary Material

I. Controlling the mass bias introduced by sulfate in Si measurements by MC-ICP-MS

The cation-exchange purification technique used here does not remove anions (in our case, mostly Cl^-, SO_4^{2-} and to a lesser extent NO_3^-) from solutions. In this case, the addition of a known artificial matrix in excess in both the sample and standard solution can be used to dilute the natural concentration of the contaminant and to homogenize sample and standard matrices (doping method, Georg et al., 2006; Hughes et al., 2011). Indeed, dissimilar matrices will affect differently the plasma and ionization efficiency and will induce artificial bias in the delta measurements, invalidating the use of the standard-sample bracketing technique.

In our samples, Cl^- originating from seawater can be neglected compared to Cl^- added as HCl (Merck Suprapur) to dissolve the brucite; and as solutions were analyzed in a HCl matrix largely in excess (up to 0.5 mol L^{-1}) compared to natural Cl^- concentration. Similarly, the occurrence of NO_3^- in seawater was resolved by the use of HNO_3 (Merck Suprapur, 0.5 mol L^{-1}) as a solvent in both the samples and standards. For KEOPS-2 surface samples, sulfate concentrations measured by ionic chromatography after purification could be significant to generate a shift in isotopic measurements (SO_4^{2-}/Si up to 20). Van den Boorn et al. (2009) has recently reported that the presence of sulfate in rock digestion solutions can induce a significant offset (up to +1.4 ‰) in silicon isotopic measurements when SO_4^{2-}/Si ratios > 0.02.

To test the effect of sulfate on silicon measurements, we doped 4 Diatomite purified solutions with variable amounts of H_2SO_4 (Merck, Suprapur) to yield solutions with SO_4^{2-}/Si ratios ranging from 0 to 19. The sulfate-doped Diatomite solutions were then analyzed for silicon isotope composition using the sulfate-free standard-sample bracketing technique. These solutions were analyzed using the same configuration as for the KEOPS-2 samples and the procedure was replicated 6 times on separated MC-ICP-MS analytical sessions.

The results of the experiment show a clear positive relation between the silicon isotopic composition of Diatomite and SO_4^{2-}/Si ratio of the solution (Fig. S1), with the increase of $\delta^{30}Si$ signatures becoming significant (+0.2 ‰) when SO_4^{2-}/Si ratios > 8. Moreover, we observe a degradation of the analytical reproducibility with increasing SO_4^{2-}/Si ratios with standard deviations up to five times higher in the most sulfate-concentrated solution, suggesting a strong decline of the measurement quality.

Doping both standard and Diatomite solutions with H_2SO_4 (final concentration 1mmol L^{-1}) would impose similar SO_4^{2-}/Si ratios in the sample and the standard solutions and should prevent any matrix effect. Indeed, we observe that the doping procedure does not induce any bias on Diatomite reference material

measurements that have a $\delta^{30}Si$ signature similar to the published values (1.27 ± 0.06 ‰, n = 50 ; compared to $\delta^{30}Si$ = 1.26 ‰, Reynolds et al., 2007).

Thus, as proposed by Hughes et al. (2011) for river waters, samples and standards solutions used for seawater isotopic analyses must be doped with sulfate when their SO_4^{2-}/Si ratios > 8 in order to control the sulfate matrix effect during MC-ICP-MS measurements. In our study, it concerned every surface samples where we used a preconcentration (MAGIC) volume > 50 ml. However, to run the MC-ICP-MS in the same matrix conditions for all samples, we decided to apply this procedure for all KEOPS-2 seawater samples. Thus, after cationic exchange purification (Georg et al., 2006) and prior to MC-ICP-MS measurements, sulfuric acid (H_4SO_4, Merck Suprapur) was added to both the standard and the samples in order to reach the same final SO_4^{2-} concentration (1 mmol L^{-1}, see Table S1).

II. Calculation of a mixed-layer deepening

The ML is subject to occasional deepening due to a variety of physical processes. Our goal here is to estimate the order of magnitude of a ML deepening that could correspond to the supply of DSi estimated from our sediment trap isotopic measurements (i.e. an increase of 7.39 µmol L^{-1}). Indeed, when the ML deepens, DSi from deeper waters is introduced to the surface. This DSi supply (or entrainment) depends therefore on three parameters: (i) the gradient of DSi concentration below the ML, (ii) the depth of the ML (H) and (iii) the depth of the deepening event (H', see Fig. S2). The variation of the ML is closely linked to the change in DSi concentration and can be explained as follows:

$$\Delta H = \frac{(DSi_t - DSi_{t0}) \times H}{DSi_{deep} - DSi_t} \qquad (1)$$

with ΔH, the change of ML depth; DSi_t and DSi_{t0}, the concentration of silicic acid in the ML before and after the mixing event respectively; and DSi_{deep}, the concentration of silicic acid below the ML.

We assume that the ML is well-homogenized with a DSi_{t0} of 9.53 µmol L^{-1} and we neglect the inverse process of "detrainment" when the water column stratifies again after the mixing event. The DSi_{deep} corresponds to the averaged WW DSi concentration estimated fro the Plateau stations (32.87 µmol L^{-1}) and the supply of DSi is estimated either from a Rayleigh model ($DSi_t - DSi_{t0}$ = 2.3 µmol L^{-1}) or from a steady state model ($DSi_t - DSi_{t0}$ = 7.39 µmol L^{-1}). Therefore, the estimated deepening of the ML is + 8.75 m or + 37 m in when we consider respectively a closed system or an open system.

References

Georg, R. B., Reynolds, B. C., Frank, M., Halliday, A. N.: New sample preparation techniques for the determination of Si isotopic compositions using MC-ICPMS, Chemical Geology, 235, 95-104, 2006.

Hughes, H. J., Delvigne, C., Korntheuer, M., De Jong, J., André, L., D. Cardinal, D.: Controlling the mass bias introduced by anionic and organic matrices in silicon isotopic measurements, Journal of Analytical Atomic Spectrometry, 26, 1892-1896, 2011.

Reynolds, B. C., Aggarwal, J., André, L., Baxter, D., Beucher, C., Brzezinski, M. A., Engström, E., Georg, R. B., Land, M., Leng, M. J., Opfergelt, S., Rodushkin, I., Sloane, H. J., van den Boorn, S. H. J. M., Vroon, P. Z., Cardinal, D.: An inter-laboratory comparison of Si isotope reference materials, Journal of Analytical Atomic Spectrometry,22, 561-568, doi:10.1039/b616755a, 2007.

Van den Boorn, S. H. J. M., Vroon, P. Z., Van Bergen, M. J.: Sulfur-induced offsets in MC-ICP-MS silicon-isotope measurements, Journal of Analytical Atomic Spectrometry, 24, 1111-1114, 2009.

Tables

Table S1: Running concentrations for isotopic analysis of seawater sample

	Si	**HCl**	**NNO_3**	**H_2SO_4**	**Mg**
Concentrations	2-2.5 ppm	0.5 mol L^{-1}	0.5 mol L^{-1}	1 mmol L^{-1}	2-2.5 ppm

Table S2: Silicic Acid, biogenic silica concentrations and $\delta^{30}Si$ of DSi and BSi for all KEOPS-2 samples. * refers to particles collected using Niskin bottles only and ** refers to particles collected with Niskin bottles and in-situ pumps.

Station	Depth (m)	$[H_4SiO_4]$ (µmol L^{-1})	δ^{30}DSi (‰)	[BSi] (µmol L^{-1})	δ^{30B}Si (‰)	
A3-1	11	22.89 ± *1.60*	1.96 ± *0.07*	1.26 ± *0.21*	0.77 ± *0.06*	*
CTD#004	42	22.83 ± *1.60*	2.01 ± *0.05*	1.35 ± *0.05*	0.82 ± *0.07*	*
20/10/2011	104	23.88 ± *1.67*	1.99 ± *0.05*	1.18 ± *0.34*	0.72 ± *0.09*	*
50°S 37.77	152	32.77 ± *2.29*	1.73 ± *0.05*	0.75 ± *0.09*	0.96 ± *0.08*	*
72°E 04.82	173	31.55 ± *2.21*	1.76 ± *0.05*	0.58 ± *0.07*	0.92 ± *0.18*	*
	204	36.41 ± *2.55*	1.71 ± *0.05*	0.51 ± *0.06*	1.21 ± *0.10*	*
	227	41.26 ± *2.89*	1.58 ± *0.05*			
	253	44.90 ± *3.14*	1.62 ± *0.05*			
	279	46.12 ± *3.23*	1.49 ± *0.05*			
	354	60.68 ± *4.25*	1.41 ± *0.05*			
	474	70.39 ± *4.93*	1.38 ± *0.05*			
TNS8	12	17.91 ± *1.25*	2.36 ± *0.05*	1.31 ± *0.27*	0.86 ± *0.05*	*
CTD#008	41	18.41 ± *1.29*		1.12 ± *0.14*	1.04 ± *0.05*	*
21/10/2011	102	19.59 ± *1.37*	2.24 ± *0.05*	1.52 ± *0.44*	0.96 ± *0.05*	*
49°S 27.77	150	21.65 ± *1.52*	2.16 ± *0.05*	1.39 ± *0.16*	1.05 ± *0.05*	*
72°E 14.41	205	26.80 ± *1.88*	1.93 ± *0.05*	1.09 ± *0.13*	1.08 ± *0.05*	*
	254	41.92 ± *2.93*	1.50 ± *0.05*			
	305	54.55 ± *3.82*	1.34 ± *0.05*			
	405	65.15 ± *4.56*	1.29 ± *0.05*			
	505	71.72 ± *5.02*	1.21 ± *0.05*			
	606	72.46 ± *5.07*				
	707	70.05 ± *4.90*	1.25 ± *0.05*			
	910	80.81 ± *5.66*	1.11 ± *0.05*			
	1000	76.33 ± *5.34*	1.24 ± *0.05*			
TNS06	11	16.42 ± *1.15*	2.41 ± *0.05*	1.38 ± *0.01*	1.11 ± *0.05*	*
CTD#10	42	16.56 ± *1.16*		1.54 ± *0.11*	1.30 ± *0.05*	*
22/10/2011	103	16.64 ± *1.16*	2.41 ± *0.05*	1.53 ± *0.01*	1.34 ± *0.05*	*
48°S 46.78	184	31.31 ± *2.19*	1.71 ± *0.05*	0.46 ± *0.05*	1.38 ± *0.05*	*
72°E 16.77	204	35.35 ± *2.47*	1.50 ± *0.05*	0.56 ± *0.06*	1.41 ± *0.05*	*
	255	43.94 ± *3.08*	1.36 ± *0.05*			
	306	52.53 ± *3.68*	1.42 ± *0.05*			
	407	61.50 ± *4.30*				
	509	69.33 ± *4.85*	1.30 ± *0.05*			
	610	73.26 ± *5.13*				
	813	80.10 ± *5.61*	1.26 ± *0.05*			
	1526	88.38 ± *6.19*	1.05 ± *0.05*			
	1886	95.96 ± *6.72*	0.95 ± *0.05*			
TNS01	11	8.96 ± *0.63*	2.32 ± *0.05*	0.24 ± *0.03*	1.35 ± *0.05*	*
CTD#15	41	8.96 ± *0.63*	2.18 ± *0.05*	0.24 ± *0.02*	1.27 ± *0.05*	*
23/10/2011	102	9.95 ± *0.70*	2.26 ± *0.05*	0.26 ± *0.03*	1.31 ± *0.05*	*
46°S 49.99	153	13.40 ± *0.94*	2.23 ± *0.11*	0.08 ± *0.01*		*
71°E 30.06	202	17.65 ± *1.24*	1.89 ± *0.05*	0.08 ± *0.01*		*
	253	26.20 ± *1.83*	1.86 ± *0.05*			
	304	32.62 ± *2.28*	1.66 ± *0.05*			
	405	45.45 ± *3.18*	1.57 ± *0.05*			
	506	54.55 ± *3.82*				
	606	57.49 ± *4.02*	1.39 ± *0.05*			
	809	71.01 ± *4.97*	1.31 ± *0.06*			
	1520	80.81 ± *5.66*	1.00 ± *0.05*			
	2282	97.60 ± *6.83*	0.90 ± *0.05*			
R2	21	12.94 ± *0.91*	2.21 ± *0.05*	0.30 ± *0.03*	0.73 ± *0.05*	*
CTD#17&20	40	12.94 ± *0.91*	2.28 ± *0.05*	0.41 ± *0.08*	0.78 ± *0.06*	*
26/10/2011	80	11.96 ± *0.84*	2.18 ± *0.05*	0.29 ± *0.03*		
50°S 21.52	90			0.93 ± *0.02*	0.96 ± *0.05*	*
66°E 43.00	100	12.98 ± *0.91*	2.27 ± *0.05*	0.27 ± *0.03*	1.18 ± *0.06*	*
	126	13.37 ± *0.94*	2.38 ± *0.05*	0.17 ± *0.02*	1.37 ± *0.05*	*
	151	12.88 ± *0.90*	2.14 ± *0.06*	0.13 ± *0.01*	1.52 ± *0.05*	*
	203	21.74 ± *1.52*	1.92 ± *0.05*	0.42 ± *0.01*	1.34 ± *0.05*	
	253	29.95 ± *2.10*	1.80 ± *0.05*			
	356	37.20 ± *2.60*	1.60 ± *0.05*			
	404	48.31 ± *3.38*	1.37 ± *0.05*			
	507	57.00 ± *3.99*	1.29 ± *0.06*	0.16 ± *0.00*	1.71 ± *0.05*	
	609	61.35 ± *4.29*	1.19 ± *0.05*	0.05 ± *0.00*	1.71 ± *0.14*	
	708		1.28 ± *0.05*			
	812	71.01 ± *4.97*	1.22 ± *0.05*	0.11 ± *0.00*	1.77 ± *0.13*	
	911	74.03 ± *5.18*	1.23 ± *0.05*			
	1011	78.27 ± *5.48*	1.08 ± *0.05*	0.05 ± *0.00*	1.85 ± *0.05*	
	1520	85.86 ± *6.01*	1.07 ± *0.05*	0.10 ± *0.00*	2.01 ± *0.10*	
	1832	90.91 ± *6.36*	1.06 ± *0.05*			
	2000			0.02 ± *0.02*		
	2473	119.57 ± *8.37*	1.13 ± *0.05*	0.08 ± *0.00*	2.09 ± *0.06*	
	2500		1.14 ± *0.05*			

Station	Depth (m)	$[H_4SiO_4]$ (µmol L^{-1})	δ^{30}DSi (‰)	[BSi] (µmol L^{-1})	δ^{30B}Si (‰)	
E1	21	15.92 ± *1.11*	2.26 ± *0.05*	1.61 ± *0.05*	1.16 ± *0.09*	*
CTD#27&30	41	15.92 ± *1.11*	2.27 ± *0.05*	1.45 ± *0.11*	1.18 ± *0.06*	*
30/10/2011	60			1.30 ± *0.09*	1.25 *0.05*	
48°S 29.88	81	8.70 ± *0.61*	2.23 ± *0.05*	1.60 ± *0.25*	1.20 ± *0.05*	*
72°E 10.66	101	16.58 ± *1.16*	2.20 ± *0.05*	1.53 ± *0.18*	1.20 ± *0.05*	**
	125	17.11 ± *1.20*	2.02 ± *0.12*	1.59 ± *0.18*	1.23 ± *0.05*	*
	151	20.32 ± *1.42*	1.99 ± *0.05*	1.42 ± *0.16*	1.30 ± *0.06*	*
	182	28.88 ± *2.02*	1.84 ± *0.06*	0.49 ± *0.06*	1.32 ± *0.05*	**
	253		1.57 ± *0.05*			
	303	52.94 ± *3.71*	1.44 ± *0.05*	0.70 ± *0.01*	1.37 ± *0.05*	
	403	63.64 ± *4.45*	1.35 ± *0.05*			
	455	70.05 ± *4.90*	1.29 ± *0.05*			
	505	70.05 ± *4.90*	1.27 ± *0.05*	0.47 ± *0.05*	1.56 ± *0.12*	
	605	76.46 ± *5.35*	1.28 ± *0.05*			
	636	76.46 ± *5.35*	1.20 ± *0.05*	0.41 ± *0.01*	1.57 ± *0.09*	
	707	76.46 ± *5.35*	1.23 ± *0.05*			
	808	80.10 ± *5.61*	1.12 ± *0.05*			
	913	80.10 ± *5.61*	1.18 ± *0.05*			
	1011	83.33 ± *5.83*	1.01 ± *0.05*	0.33 ± *0.03*	1.71 ± *0.05*	
	1498	88.38 ± *6.19*	0.98 ± *0.05*	0.22 ± *0.01*	1.74 ± *0.05*	
	1780			0.20 ± *0.00*	1.79 ± *0.05*	
	2042	101.06 ± *7.07*	1.18 ± *0.05*	0.52 ± *0.01*	1.83 ± *0.12*	
TEW1	10	7.46 ± *0.52*	2.75 ± *0.05*	6.33 ± *0.55*	2.04 ± *0.05*	*
CTD#35	31	12.94 ± *0.91*	2.39 ± *0.06*	3.30 ± *0.24*	1.86 ± *0.05*	*
31/10/2011	51	14.93 ± *1.04*	2.16 ± *0.05*	2.75 ±		*
49°S 08.99	71	16.42 ± *1.15*	2.19 ± *0.05*	1.88 ± *0.01*	1.66 ± *0.05*	*
69°E 50.01	80		1.88 ± *0.05*			
TEW3	16	19.90 ± *1.39*		0.63 ± *0.01*	0.47 ± *0.05*	*
CTD#38	41	19.90 ± *1.39*	2.31 ± *0.05*	0.92 ± *0.08*	0.79 ± *0.05*	*
31/10/2011	61	11.96 ± *0.84*	2.33 ± *0.05*	0.78 ± *0.09*	0.57 ± *0.05*	*
48°S 47.95	76	8.70 ± *0.61*	2.01 ± *0.05*	0.70 ± *0.08*	0.56 ± *0.05*	*
71°E 01.06	111	24.74 ± *1.73*	1.86 ± *0.05*	0.56 ± *0.06*	0.74 ± *0.05*	*
	183	28.34 ± *1.98*		0.39 ± *0.04*	1.26 ± *0.05*	*
	253	40.11 ± *2.81*				
	277	41.18 ± *2.88*	1.58 ± *0.05*			
	404	58.82 ± *4.12*				
	545	75.14 ± *5.26*	1.41 ± *0.05*			
E2	11	11.96 ± *0.84*	2.34 ± *0.06*	1.87 ± *0.05*	1.23 ± *0.05*	*
CTD#43	41	18.41 ± *1.29*	2.42 ± *0.12*	1.00 ± *0.04*	1.27 ± *0.06*	*
01/11/2011	102	17.65 ± *1.24*	2.22 ± *0.05*	1.14 ± *0.02*	1.21 ± *0.05*	*
48°S 31.41	153	20.32 ± *1.42*	1.99 ± *0.05*	0.96 ± *0.11*	1.25 ± *0.05*	*
72°E 04.63	204	46.01 ± *3.22*		0.48 ± *0.06*	1.42 ± *0.09*	*
	254	36.36 ± *2.55*	1.80 ± *0.05*			
	305	58.82 ± *4.12*				
	406	68.98 ± *4.83*	1.30 ± *0.05*			
	507	73.80 ± *5.17*				
	609	75.24 ± *5.27*	1.22 ± *0.05*			
	813	72.95 ± *5.11*	1.21 ± *0.05*			
	1016	83.33 ± *5.83*	1.08 ± *0.05*			
	2020	75.24 ± *5.27*	0.93 ± *0.05*			
TEW8	10	6.97 ± *0.49*		2.58 ± *0.33*	1.57 ± *0.05*	*
CTD#47	41	11.44 ± *0.80*	2.47 ± *0.05*	2.33 ± *0.31*	1.62 ± *0.05*	*
02/11/2011	102	20.62 ± *1.44*	2.08 ± *0.05*	0.74 ± *0.12*	1.34 ± *0.05*	*
48°S 28.05	152	23.71 ± *1.66*	1.89 ± *0.05*	0.47 ± *0.05*	1.34 ± *0.05*	*
75°E 00.19	202	26.20 ± *1.83*	1.79 ± *0.05*	0.22 ± *0.03*	1.38 ± *0.05*	*
	254	32.09 ± *2.25*	1.66 ± *0.05*			
	304	37.97 ± *2.66*	1.48 ± *0.05*			
	405	53.48 ± *3.74*	1.45 ± *0.05*			
	507	57.67 ± *4.04*				
	609	66.87 ± *4.68*	1.40 ± *0.05*			
	809	66.67 ± *4.67*	1.33 ± *0.05*			
	1011	76.07 ± *5.33*				
	2812	133.84 ± *9.37*	1.07 ± *0.05*			

Station	Depth (m)	$[H_4SiO_4]$ (µmol L^{-1})	δ^{30}DSi (‰)	[BSi] (µmol L^{-1})	δ^{30B}Si (‰)	
E3	11	15.42 ± *1.08*	2.40 ± *0.11*	1.22 ± *0.03*	1.12 ± *0.05*	*
CTD#50&55	42	15.42 ± *1.08*	2.29 ± *0.05*	1.54 ± *0.18*	1.12 ± *0.05*	*
04/11/2011				1.98 ± *0.19*		
48°S 42.07	71	17.91 ± *1.25*	2.16 ± *0.05*	1.19 ± *0.14*	1.26 ± *0.09*	*
71°E 58.02	102	22.83 ± *1.60*	2.15 ± *0.05*	0.81 ± *0.09*	1.35 ± *0.05*	*
	125	17.79 ± *1.25*		1.83 ± *0.21*	1.33 ± *0.05*	*
	153	19.25 ± *1.35*	2.06 ± *0.05*	1.33 ± *0.15*	1.30 ± *0.05*	*
	203	28.88 ± *2.02*	1.92 ± *0.05*	0.42 ± *0.05*	1.35 ± *0.05*	*
	225			0.58 ± *0.01*	1.45 ± *0.05*	*
	252	40.64 ± *2.84*	1.63 ± *0.05*			
	304	49.28 ± *3.45*	1.32 ± *0.05*			
	404	69.36 ± *4.86*	1.23 ± *0.07*	0.38 ± *0.01*	1.51 ± *0.05*	
	505	69.57 ± *4.87*	1.36 ± *0.05*			
	606	74.03 ± *5.18*	1.25 ± *0.05*	0.46 ± *0.02*	1.58 ± *0.06*	
	707	78.88 ± *5.52*	1.26 ± *0.05*			
	800	82.52 ± *5.78*		0.17 ± *0.02*	1.66 ± *0.05*	
	910	82.52 ± *5.78*	1.24 ± *0.07*			
	1012	77.88 ± *5.45*	1.16 ± *0.05*	0.27 ± *0.01*	1.68 ± *0.06*	
	1214	78.85 ± *5.52*	1.24 ± *0.18*	0.26 ± *0.01*	1.63 ± *0.07*	
	1500			0.22 ± *0.01*	1.70 ± *0.05*	
	1908	82.52 ± *5.78*	1.06 ± *0.05*			
	2000		1.12 ± *0.05*			
F-L	11	7.61 ± *0.53*	2.72 ± *0.05*	3.00 ± *0.28*	1.56 ± *0.18*	*
CTD#63&68	35	8.70 ± *0.61*	2.53 ± *0.08*	3.54 ± *0.26*	1.60 ± *0.05*	*
07/11/2011	55			1.88 ± *0.16*	1.66 ± *0.05*	
48°S 37.27	61	9.95 ± *0.70*	2.39 ± *0.05*	2.33 ± *0.80*	1.59 ± *0.05*	*
74°E 48.44	80	14.42 ± *1.01*	2.12 ± *0.07*	0.51 ± *0.06*	1.38 ± *0.05*	*
	101	17.79 ± *1.25*	1.97 ± *0.05*	0.34 ± *0.03*	1.49 ± *0.05*	**
	126	19.71 ± *1.38*	1.97 ± *0.05*	0.23 ± *0.03*	1.50 ± *0.05*	*
	151	21.15 ± *1.48*	1.66 ± *0.05*	0.24 ± *0.03*	1.44 ± *0.05*	*
	202		1.66 ± *0.05*			
	225			0.13 ± *0.01*	1.55 ± *0.09*	
	252	31.40 ± *2.20*	1.71 ± *0.05*			
	303	37.20 ± *2.60*	1.51 ± *0.05*			
	404	46.86 ± *3.28*	1.31 ± *0.08*	0.14 ± *0.00*	1.68 ± *0.05*	
	506	63.19 ± *4.42*	1.24 ± *0.05*			
	607	60.87 ± *4.26*	1.28 ± *0.05*	0.14 ± *0.00*	1.74 ± *0.05*	
	707	70.39 ± *4.93*	1.25 ± *0.05*			
	911	76.46 ± *5.35*	1.25 ± *0.05*			
	1013	71.01 ± *4.97*	1.26 ± *0.05*			
	1215	72.46 ± *5.07*	1.26 ± *0.05*	0.22 ± *0.00*	1.84 ± *0.05*	
	1772	101.94 ± *7.14*	1.04 ± *0.05*	0.17 ± *0.01*	1.86 ± *0.07*	
	2200			0.23 ± *0.00*	1.90 ± *0.09*	
	2741	135.36 ± *9.48*	1.10 ± *0.05*			
	3000		1.16 ± *0.05*			
E4W	10	11.96 ± *0.84*	2.26 ± *0.05*	3.88 ± *0.22*	0.93 ± *0.10*	*
CTD#81&87	41	18.91 ± *1.32*	2.22 ± *0.05*	3.92 ± *0.57*	0.75 ± *0.07*	*
12/11/2011	70	20.90 ± *1.46*	2.20 ± *0.05*	1.91 ± *0.41*	0.69 ± *0.05*	*
48°S 45.93	94	24.64 ± *1.72*	1.94 ± *0.05*	0.43 ± *0.05*	0.70 ± *0.05*	*
71°E 25.50	126	24.15 ± *1.69*	1.89 ± *0.05*	0.38 ± *0.04*	0.82 ± *0.05*	*
	153	24.64 ± *1.72*	1.78 ± *0.05*	0.72 ± *0.08*	1.05 ± *0.05*	*
	175			0.79 ± *0.00*	1.11 ± *0.05*	
	203	36.71 ± *2.57*	1.67 ± *0.05*	±		
	252	45.89 ± *3.21*	1.42 ± *0.05*	±		
	304	49.76 ± *3.48*	1.39 ± *0.11*	0.62 ± *0.01*	1.48 ± *0.05*	
	406	61.35 ± *4.29*	1.28 ± *0.05*			
	453	67.63 ± *4.73*	1.32 ± *0.05*			
	507	68.60 ± *4.80*				
	607	75.24 ± *5.27*	1.22 ± *0.05*	0.63 ± *0.03*	1.70 ± *0.08*	
	708	76.46 ± *5.35*	1.29 ± *0.05*			
	811	77.67 ± *5.44*	1.32 ± *0.10*	0.60 ± *0.06*	1.67 ± *0.05*	
	909	76.46 ± *5.35*	1.25 ± *0.08*			
	1011	81.31 ± *5.69*	1.20 ± *0.05*			
	1214	97.09 ± *6.80*	1.01 ± *0.05*			
	1384	101.94 ± *7.14*	1.01 ± *0.05*			

Station	Depth (m)	$[H_4SiO_4]$ (µmol L^{-1})	δ^{30}DSi (‰)	[BSi] (µmol L^{-1})	δ^{30B}Si (‰)	
E4E	20	12.44 ± *0.87*	2.48 ± *0.05*	2.94 ± *0.05*	1.32 ± *0.06*	*
CTD#94&97	51	8.70 ± *0.61*	2.57 ± *0.05*	2.43 ± *0.43*	1.40 ± *0.05*	*
14/11/2011	93	18.41 ± *1.29*	2.25 ± *0.05*	2.31 ± *0.39*	1.46 ± *0.06*	*
48°S 42.93	103	20.62 ± *1.44*	2.21 ± *0.05*	0.67 ± *0.08*	1.35 ± *0.05*	*
72°E 33.76	126	22.68 ± *1.59*	2.14 ± *0.05*	0.75 ± *0.09*	1.39 ± *0.05*	*
	152	24.74 ± *1.73*	1.83 ± *0.05*	0.69 ± *0.08*	1.28 ± *0.05*	*
	181	27.81 ± *1.95*	1.80 ± *0.05*			
	253	49.73 ± *3.48*	1.53 ± *0.05*			
	303	54.01 ± *3.78*	1.45 ± *0.05*			
	404	64.71 ± *4.53*	1.35 ± *0.05*			
	505	75.72 ± *5.30*	1.21 ± *0.05*			
	606	74.03 ± *5.18*	1.29 ± *0.05*			
	706	78.88 ± *5.52*	1.24 ± *0.05*			
	912	77.67 ± *5.44*	1.20 ± *0.05*			
	1012	80.10 ± *5.61*	1.18 ± *0.10*			
	1265	83.74 ± *5.86*	1.16 ± *0.05*			
	1518	89.81 ± *6.29*	1.11 ± *0.05*			
	1827	95.87 ± *6.71*	1.09 ± *0.05*			
	2027	89.81 ± *6.29*	0.97 ± *0.05*			
	2212	91.41 ± *6.40*	1.21 ± *0.06*			
A3-2	11	19.40 ± *1.36*	2.11 ± *0.05*	3.83 ± *0.49*	1.01 ± *0.05*	*
CTD#107	40	19.40 ± *1.36*	2.10 ± *0.06*	4.06 ± *0.42*	0.93 ± *0.05*	**
16/11/2011	81	20.40 ± *1.43*	2.07 ± *0.05*	3.55 ± *0.36*	0.92 ± *0.07*	*
50°S 37.46	126	19.71 ± *1.38*	2.11 ± *0.05*	4.33 ± *0.83*	1.00 ± *0.05*	*
72°E 03.34	150	19.71 ± *1.38*	1.92 ± *0.05*	3.58 ± *0.26*	1.03 ± *0.05*	**
	176	24.60 ± *1.72*	1.89 ± *0.05*	2.04 ± *0.31*	1.01 ± *0.09*	*
	202	31.90 ± *2.23*	1.69 ± *0.05*	0.85 ± *0.06*	1.02 ± *0.08*	*
	270	40.64 ± *2.84*	1.62 ± *0.05*	0.72 ± *0.14*	1.34 ± *0.07*	
	303	45.45 ± *3.18*	1.51 ± *0.05*			
	350			0.82 ± *0.09*	1.49 ± *0.09*	
	405	63.10 ± *4.42*	1.45 *0.05*			
	460			3.09 ± *0.02*	1.72 ± *0.05*	
	513	80.21 ± *5.61*	1.34 *0.05*			
E5	11	12.94 ± *0.91*	2.44 ± *0.10*	1.75 ± *0.19*	1.26 ± *0.05*	*
CTD#113&114	41	12.94 ± *0.91*	2.58 ± *0.05*	3.44 ± *1.46*	1.39 ± *0.05*	*
18/11/2011	55			1.64 ± *0.04*		
48°S 24.69	82	12.94 ± *0.91*	2.36 ± *0.05*	2.44 ± *0.07*	1.46 ± *0.08*	*
71°E 53.99	102	21.39 ± *1.50*		0.95 ± *0.11*	1.41 ± *0.05*	**
	126	18.01 ± *1.26*		0.73 ± *0.08*	1.44 ± *0.05*	*
	152	23.12 ± *1.62*		0.66 ± *0.08*	1.37 ± *0.05*	*
	202	22.75 ± *1.59*	2.12 ± *0.05*			
	220			1.01 ± *0.04*	1.40 ± *0.05*	
	252	38.65 ± *2.71*	1.66 ± *0.05*			
	302	50.24 ± *3.52*	1.49 ± *0.05*			
	404	62.32 ± *4.36*	1.37 ± *0.05*	2.30 ± *0.08*	1.43 ± *0.05*	
	507	69.08 ± *4.84*	1.48 ± *0.05*			
	606	71.50 ± *5.00*	1.41 ± *0.05*			
	707	84.39 ± *5.91*	1.20 ± *0.05*			
	800			0.35 ± *0.01*	1.62 ± *0.05*	
	911	90.17 ± *6.31*	1.20 ± *0.05*			
	1011	88.44 ± *6.19*	1.23 ± *0.05*	0.25 ± *0.02*	1.66 ± *0.08*	
	1214	88.24 ± *6.18*	1.15 ± *0.05*			
	1500			0.17 ± *0.02*	1.69 ± *0.09*	
	1922	112.72 ± *7.89*	1.11 ± *0.05*			

Table S3: Neptune+ MC-ICP-MS operating conditions

Resolution	Medium
Forward Power	1200 W
Accelerating Voltage	10 kV
Plasma Mode	Dry Plasma
Cool Gas Flow Rate	16 L min^{-1}
Auxiliary Gas Flow Rate	1.1-1.4 L min^{-1}
Sample Gas Flow Rate	0.9-1 L min^{-1}
Cones Type	Nickel X-Skimmer cone + Standard Ni-Sample cone
Desolvator	Apex (ESI)
Nebulizer	PFA microcentric nebuliser 100 µL min^{-1}
Running Concentrations	Si = 2-2.5 ppm, Mg = 2-2.5 ppm
Sensitivity	3-4 V ppm^{-1}
Blank Level	< 1% signal
^{30}Si Interference	< 30 mV (usually 10-15 mV)

Table S4: Central values of DSi concentrations (µmol L^{-1}) and $\delta^{30}Si_{DSi}$ signatures (‰) for different water masses across the Kerguelen Plateau region (ML: Mixed Layer; WW: Winter Water; UCDW: Upper Circumpolar Deep Water; LCDW: Lower Circumpolar Deep Water; AABW: Anatarctic Bottom Water). Except for the WW, median and interquartile range represent the "central values" and dispersion for the water masses. Since they displayed the strongest gradient of values, the WW Si-properties were defined using the threshold salinity method (see text for further details).

Station	CTD #	ML		WW		UCDW		LCDW		AABW	
		$[H_4SiO_4]$ (µmol L^{-1})	$\delta^{30}Si_{DSi}$ (‰)	$[H_4SiO_4]$ (µmol L^{-1})	$\delta^{30}Si_{DSi}$ (‰)	$[H_4SiO_4]$ (µmol L^{-1})	$\delta^{30}Si_{DSi}$ (‰)	$[H_4SiO_4]$ (µmol L^{-1})	$\delta^{30}Si_{DSi}$ (‰)	$[H_4SiO_4]$ (µmol L^{-1})	$\delta^{30}Si_{DSi}$ (‰)
A3-1	4	23.38 ± *3.23*	1.97 ± *0.09*	31.55 ± *2.21*	1.76 ± *0.05*	70.39 ± *0.00*	1.38 ± *0.00*				
TNS08	8	19.00 ± *1.82*	2.24 ± *0.10*	26.80 ± *1.88*	1.93 ± *0.05*	72.46 ± *4.61*	1.22 ± *0.05*				
TNS06	10	16.56 ± *0.11*	2.41 ± *0.00*	31.31 ± *2.19*	1.71 ± *0.05*	73.26 ± *5.39*	1.28 ± *0.02*	92.17 ± *3.79*	1.00 ± *0.05*		
TNS01	15	8.96 ± *0.50*	2.26 ± *0.07*	13.40 ± *0.94*	2.23 ± *0.11*	57.49 ± *8.23*	1.35 ± *0.04*	89.20 ± *8.39*	1.01 ± *0.01*		
R2	17	12.94 ± *0.07*	2.24 ± *0.09*	21.74 ± *1.52*	1.92 ± *0.05*	66.18 ± *15.18*	1.23 ± *0.08*	90.91 ± *16.85*	1.10 ± *0.07*		
E1	27	16.25 ± *1.06*	2.21 ± *0.18*	28.88 ± *2.02*	1.84 ± *0.06*	76.46 ± *5.24*	1.22 ± *0.11*	94.72 ± *6.34*	1.08 ± *0.10*		
TEW1	35	13.93 ± *3.73*	2.19 ± *0.22*								
TEW3	38	19.90 ± *7.94*	2.16 ± *0.34*	24.74 ± *1.73*	1.86 ± *0.05*	75.14 ± *0.00*	1.41 ± *0.02*				
E2	43	18.03 ± *2.66*	2.28 ± *0.20*	20.32 ± *1.42*	1.99 ± *0.05*	73.80 ± *2.30*	1.21 ± *0.14*	75.24 ± *0.00*	0.93 ± *0.04*		
TEW8	47	9.20 ± *2.24*	2.47 ± *0.03*	20.62 ± *1.44*	2.08 ± *0.05*	66.67 ± *9.20*	1.40 ± *0.06*	133.84 ± *0.00*	1.07 ± *0.00*		
E3	50	17.85 ± *2.90*	2.16 ± *0.14*	28.88 ± *2.02*	1.92 ± *0.05*	78.85 ± *4.75*	1.24 ± *0.06*	82.52 ± *0.00*	1.09 ± *0.03*		
FL	63	8.70 ± *1.17*	2.53 ± *0.16*	14.42 ± *1.01*	2.12 ± *0.07*	70.70 ± *7.11*	1.26 ± *0.01*	101.94 ± *0.00*	1.04 ± *0.04*	135.36 ± *0.00*	1.13 ± *0.03*
E4W	81	22.53 ± *5.11*	2.07 ± *0.01*	36.71 ± *2.57*	1.67 ± *0.05*	76.46 ± *5.00*	1.25 ± *0.07*	101.94 ± *0.00*	1.01 ± *0.03*		
E4E	94	15.42 ± *7.46*	2.36 ± *0.26*	22.68 ± *1.59*	2.14 ± *0.05*	78.28 ± *3.58*	1.20 ± *0.05*	90.61 ± *2.72*	1.10 ± *0.08*		
A3-2	107	19.71 ± *0.31*	2.10 ± *0.04*	31.90 ± *2.23*	1.69 ± *0.05*	71.66 ± *8.56*	1.39 ± *0.05*				
E5	114	12.94 ± *2.11*	2.44 ± *0.11*	22.75 ± *1.59*	2.12 ± *0.05*	86.31 ± *13.67*	1.21 ± *0.13*	112.72 ± *0.00*	1.11 ± *0.04*		

Figure captions

Figure S1: Effect of sulfate (expressed as SO_4^{2-}/Si ratios) on silicon isotope measurements ($\Delta\delta^{30}Si$ = offset in $\delta^{30}Si$ of sulfate-doped Diatomite relative to pure standard). Error bars represent 1sd. Black dashed and red dotted lines are the + 1 sd and + 2 sd from the initial (non-doped) value, respectively.

Figure S2: Schematic representation of entrainment and its impact on DSi concentration in the mixed layer. Grey dotted line and dark strait line correspond to the conditions before and after the mixing event, respectively.

Figure S3: $\delta^{29}Si$ versus $\delta^{30}Si$ of samples measured by Neptune+ MC-ICP-MS in dry plasma mode. DSi samples are in blue, surface BSi samples (collected using nuclepore membrane filtration) are in green, and deep BSi samples (collected with in situ pumps) are in black. Error bars represent the average standard deviation of duplicates (±1 sd) and the line shows the theoretical kinetic fractionation law between ^{29}Si and ^{30}Si (y = 0.51x, as calculated following Young et al., 2002).

Figure S4: All KEOPS-2 (black diamonds) and KEOPS-1 (grey crosses) silicic acid $\delta^{30}Si$ plotted against the silicic acid concentration (a.) and deep KEOPS-2 and KEOPS-1 silicic acid $\delta^{30}Si$ plotted against $1/[H_4SiO_4]$. The equations of the two curves are given and numbers in brackets are the standard deviations (1sd) of the slope and the intercept, respectively.

Figure S5: Potential temperature – salinity (θ-S) diagram for all KEOPS-2 stations.

Figures

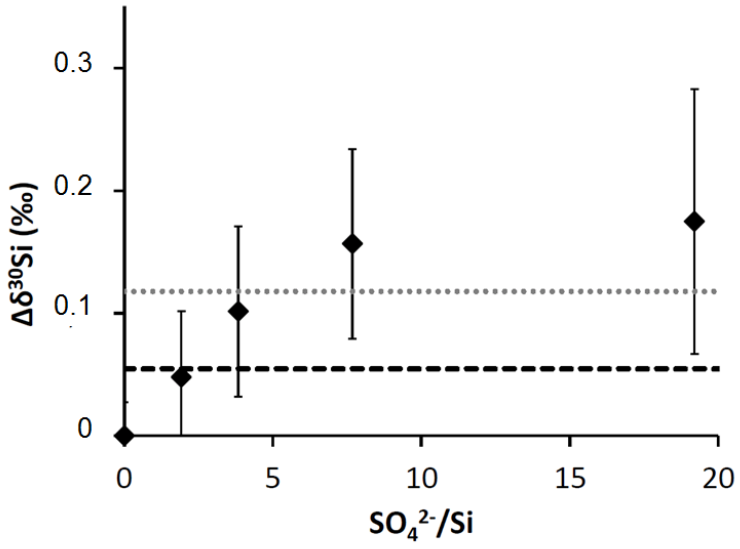

Figure S1

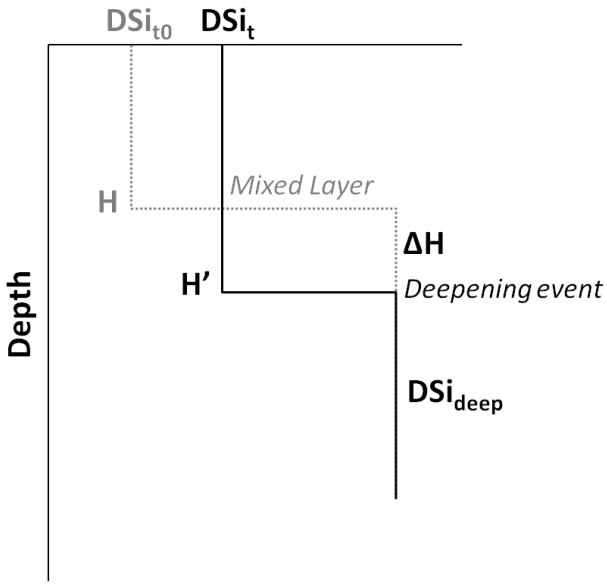

Figure S2

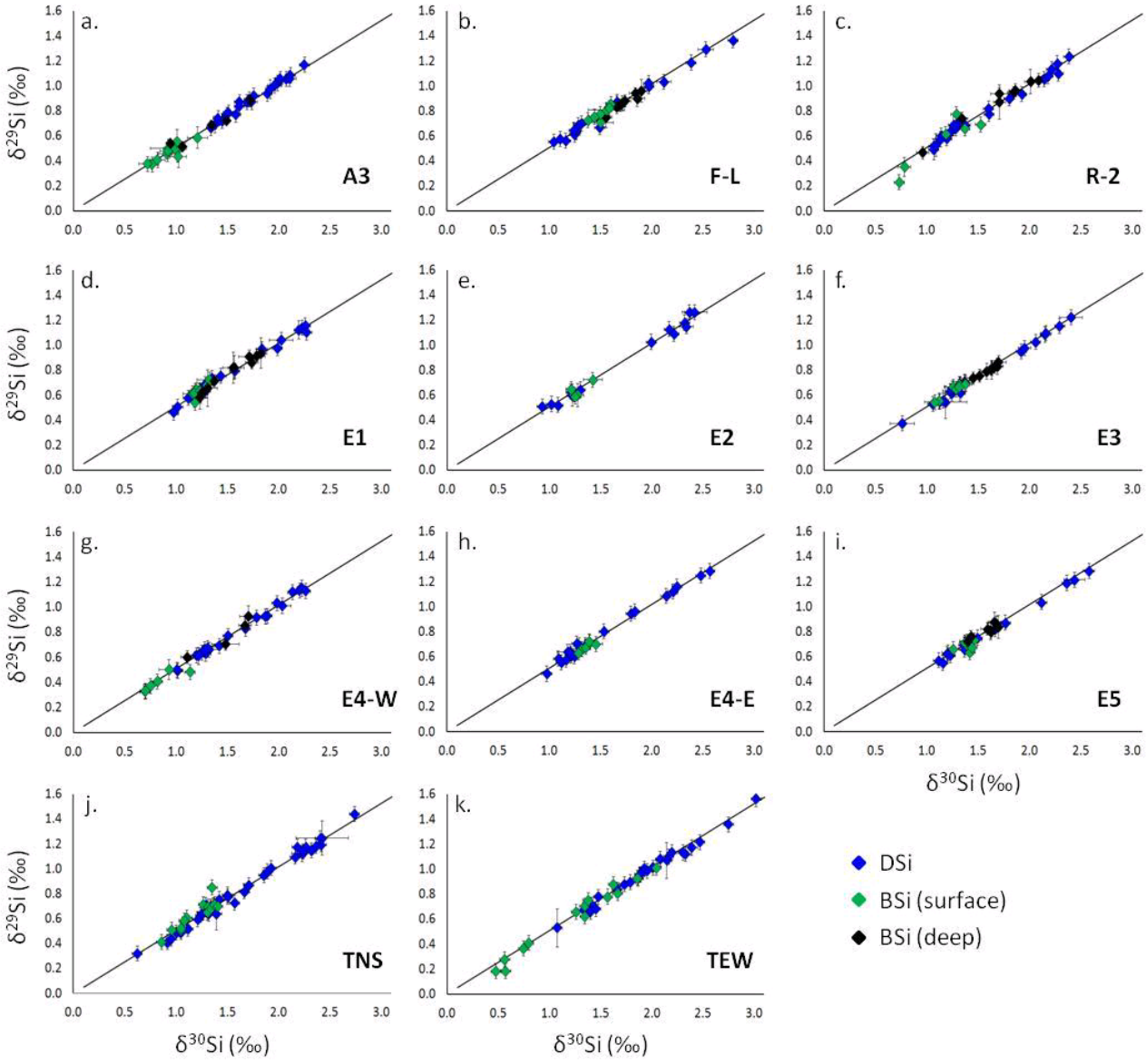

Figure S3

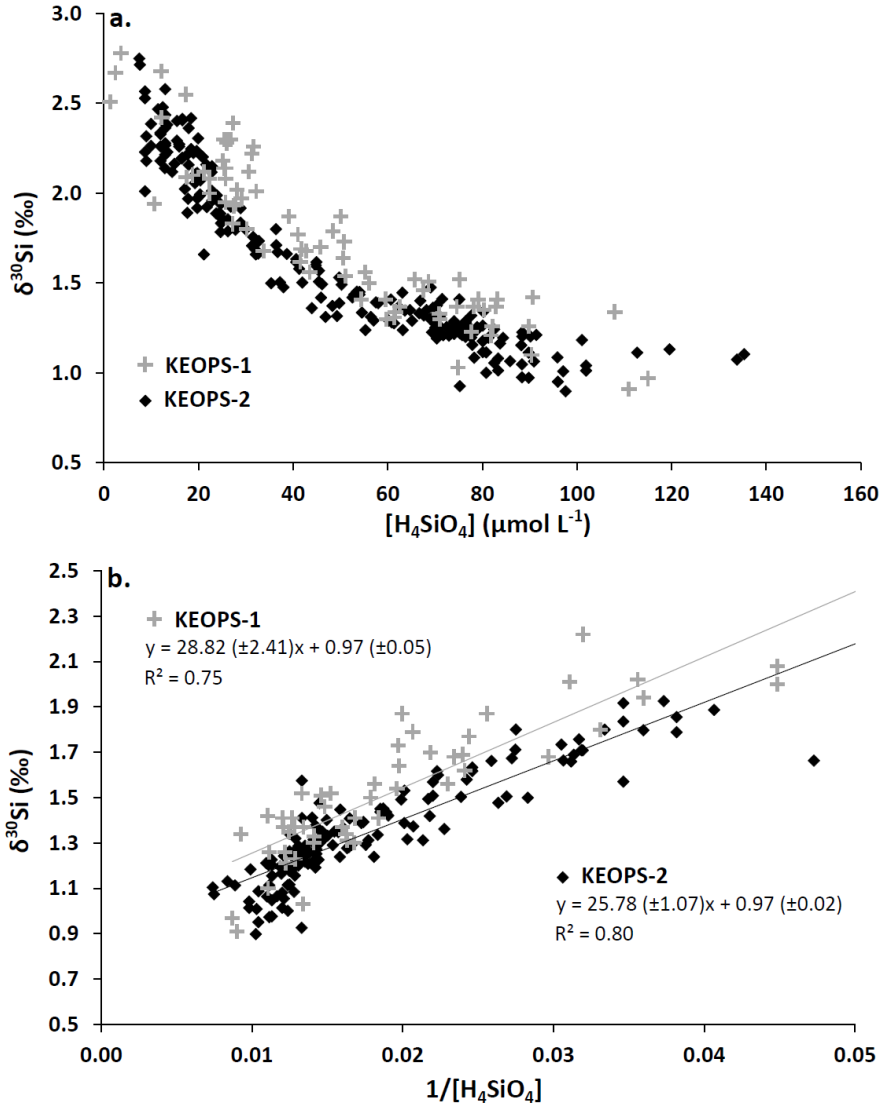
a.
3.0
2.5
2.0
1.5
1.0
0.5
δ30Si (‰)
KEOPS-1
KEOPS-2
0
20
40
60
80
100
120
140
160
[H4SiO4] (µmol L-1)
b.
KEOPS-1
y = 28.82 (±2.41)x + 0.97 (±0.05)
R² = 0.75
KEOPS-2
y = 25.78 (±1.07)x + 0.97 (±0.02)
R² = 0.80
2.5
2.3
2.1
1.9
1.7
1.5
1.3
1.1
0.9
0.7
0.5
δ30Si (‰)
0.00
0.01
0.02
0.03
0.04
0.05
1/[H4SiO4]

Figure S4

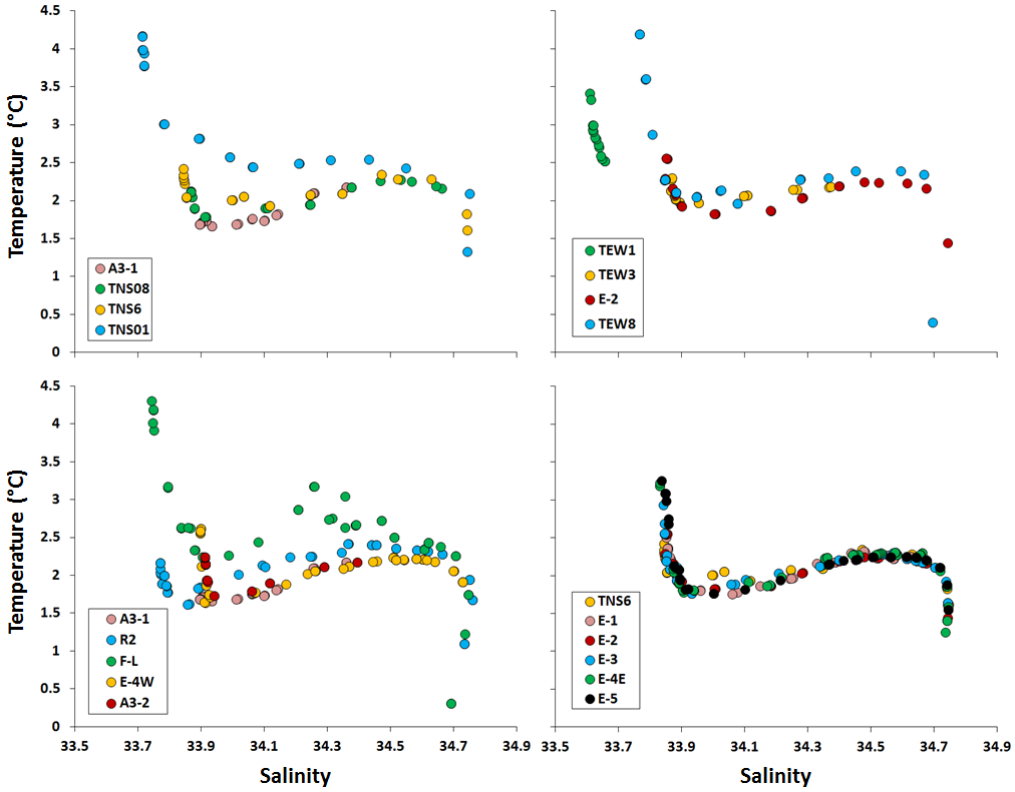
Temperature (°C)
Salinity
A3-1
TNS08
TNS6
TNS01
TEW1
TEW3
E-2
TEW8
A3-1
R2
F-L
E-4W
A3-2
TNS6
E-1
E-2
E-3
E-4E
E-5

Figure S5